Preliminary crystallographic study of turkey gizzard vinculin

O. Kogan,[a]* A. Yarden,[b] M. Gimona,[c] B. Geiger[b] and M. Safro[a]

[a]Department of Structural Biology, Weizmann Institute of Science, Rehovot, Israel, [b]Department of Molecular Cell Biology, Weizmann Institute of Science, Rehovot, Israel, and [c]Department of Cell Biology, Institute of Molecular Biology, Austrian Academy of Science, A-5020, Salzburg, Austria

Correspondence e-mail:
mark.safro@weizmann.ac.il

Vinculin is a 117 kDa microfilament-associated protein located at the cytoplasmic aspects of focal contacts and cell–cell adherens type junctions. In both sites, vinculin participates in the formation of a submembrane 'plaque' structure which is responsible for the attachment of actin filaments to the plasma membrane. Vinculin consists of 1066 amino acids, which form a large 90 kDa globular head domain and a rod-like 29 kDa tail domain. The two domains are separated by several stretches of proline residues where the major proteolytic cleavage sites are located. The experimental procedure for isolation and purification of vinculin from smooth muscle has been developed and crystals of native vinculin suitable for X-ray analysis have been obtained. The homogeneity of the vinculin solution was analyzed prior to crystallization using dynamic light scattering. Crystals of vinculin have been obtained in buffer containing 2 mg ml^{-1} protein, 0.9 M ammonium sulfate, 0.1 M MES pH 6.5 using both the hanging-drop and sitting-drop vapour-diffusion methods. The crystals have the form of rhombic plates and grow to maximal dimensions of $0.3 \times 0.3 \times 0.05$ mm in two weeks. Preliminary X-ray data show that the crystals diffract to 3.5 Å resolution at the X11 beamline of DESY and belong to the monoclinic space group $P2_1$. Crystal unit-cell parameters are estimated to be $a = 57$, $b = 351$, $c = 70$ Å, $\alpha = 90$, $\beta = 113$, $\gamma = 90°$.

1. Introduction

Formation of contacts with neighbouring cells and with the extracellular matrix (ECM) is a prerequisite in multicellular organisms for many fundamental processes such as morphogenesis, maintenance of tissue integrity, wound healing and cell growth and motility. Cell contacts are associated with the actin cytoskeleton *via* multiprotein assemblies of anchor proteins that link the transmembrane adhesion receptors to the actin network.

Vinculin is one of the central proteins in this assembly (Geiger *et al.*, 1980; Otto, 1990) and was first isolated from chicken gizzard (Geiger, 1979) and later shown to be in all actin-associated adhesion (cell–cell and cell–ECM) sites. Tissue surveys confirmed that vinculin is indeed a ubiquitous protein present in a wide variety of cell types, including many mesenchymal and epithelial cells as well as in lymphoid cells and platelets (Koteliansky *et al.*, 1984; Takubo *et al.*, 1998; Hirsch *et al.*, 1994).

Vinculin is encoded by a single copy gene and its cDNA derived from different sources, including chicken (Price *et al.*, 1987, 1989; Coutu & Craig, 1988), human (Weller *et al.*, 1990), mouse (Ben-Zeev *et al.*, 1990) and *Caenorhabditis elegans* (Barstead & Water-

ston, 1989), has been cloned and sequenced. These studies combined with biochemical and electron-microscopic analysis indicated that vinculin is a protein of 1066 amino acids with molecular weight of ~117 kDa (Price *et al.*, 1989). The molecule consists of a large 90 kDa globular 'head' domain and a rod-like 32 kDa 'tail' domain. V8 and other proteases cleave the molecule at a hinge region which is located between these two domains and is enriched with proline residues. It was further shown that the vinculin molecule exists in a 'closed' and an 'open' conformation. The transition into the active 'open' conformation which allows vinculin to bind to other cytoskeletal components is triggered by binding of the signalling molecule phosphatidylinositol-4,5-biphosphate (PIP$_2$) to two discrete sequence stretches in the vinculin tail, thereby disrupting the head-to-tail interaction. It was also reported that serine/threonine phosphorylation exerts some influence on the intramolecular head-to-tail interactions (Schwienbacher *et al.*, 1996).

Vinculin is a multiligand protein and can interact with a large number of partner proteins through several domains that have been mapped. Biochemical experiments showed that vinculin binds *via* its NH$_2$-terminus to talin (Burridge & Mangeat, 1984)

and to α-actinin (Kroemker *et al.*, 1994). The hinge region provides the necessary flexibility in the process of vinculin activation and contains a tyrosine phosphorylation site (residue 822) where post-translational modification by pp60[src] occurs (Sefton *et al.*, 1981). The proline-rich regions (837–847, 860–878) bind to the vasodilator-stimulated phosphoprotein (VASP; Brindle *et al.*, 1996). Two additional vinculin-binding proteins have been identified recently: vinexin and ponsin (Mandai *et al.*, 1999; Kioka *et al.*, 1999). It is noteworthy that in addition to the formation of intermolecular contacts with other proteins, vinculin was reported to bind to other vinculin molecules, forming oligomers (Molony & Burridge, 1985).

The COOH-terminal tail region of vinculin contains binding sites for paxillin (residues 978–1000; Turner *et al.*, 1990), acidic phospholipids (residues 935–978, 1020–1040; Johnson & Craig, 1995) and F-actin (residues 893–985 and 1016–1066; Molony & Burridge, 1985). The isolated tail fragment contains a salt-sensitive binding site for acidic phospholipids. Since native vinculin binds poorly to acidic phospholipids in buffers with physiological ionic strength, it was proposed that regulated exposure of this phospholipid-binding site might play a role in recruitment or retention of vinculin at the plasma membrane (Johnson *et al.*, 1998). Interaction of vinculin with membrane phospholipids, directed by unmasking of the acidic phospholipid-binding site, could stabilize vinculin's localization at the plasma membrane and facilitate its interaction with other junctional components. Association of vinculin with the membrane could also lead to partial insertion of the protein into the lipid bilayer, possibly strengthening the connection between the cytoplasmic adhesion complex and the membrane. The crystal structure of C-terminal fragment 879–1066 of vinculin has recently been solved (Bakolista *et al.*, 1999). It comprises a five-helix bundle 60 Å long and ∼25 Å in diameter which can deeply penetrate into acidic phospholipid bilayers. All five helices are markedly amphipathic, exposing their hydrophobic side chains into the hydrophobic interior of the bundle and with their hydrophilic side chains pointing outward.

Characterization of the structure of entire vinculin at the atomic level will provide valuable information on vinculin conformational states and on its mode of interaction with various partner proteins at cell adhesion sites. Based on the atomic coordinates of the vinculin molecule and using biochemical modification approaches and a battery of recombinant vinculin mutants we intend to clarify the role of vinculin in the linkage of the cytoskeleton and signalling molecules to the membrane at cell adhesions and thus to elucidate the structural organization of the junctional plaque.

2. Experimental procedure

2.1. Purification

The extraction of vinculin from turkey gizzard smooth muscle was carried out using a modified protocol of Gimona *et al.* (1987). Fresh muscle, obtained 3–4 h after slaughter and transported on ice, was cleaned, freed of connecting tissue, minced and blended at top speed in the cold in a Sorvall Omnimixer with a buffer containing 20 mM KCl, 20 mM imidazole, 0.5 mM DTE (dithioerythritol), 0.5 mM PMSF (phenylmethylsulfonyl fluoride) pH 6.8. Typically, 900 g of muscle was resuspended in a total volume of 3.6 l. Subsequently, the extract was subjected to homogenization in 300 ml glass–Teflon homogenizer. After centrifugation, the pellet was subjected to two additional cycles of homogenization and washing steps and used for further extractions. To remove myosin and actin, this pellet was resuspended in a low-salt extraction solution {40 mM KCl, 20 mM imidazole, 2 mM EDTA (ethylenedinitrilo tetraacetic acid), 2 mM EGTA [ethylene glycol-bis (β-aminoethyl ether)-N,N,N',N'-tetraacetic acid], 10 mM ATP (adenosine 5′-triphosphate), 1 mM DTE, 1 mM PMSF pH 7.0}, blended in a Sorvall Omnimixer in a total volume of 3.6 l and centrifuged at 15 000g for 45 min. The pellet was then resuspended in 3–5 l of potassium iodide extraction buffer (1 M KI, 20 mM imidazole, 2 mM EDTA, 2 mM EGTA, 100 mg ml^{-1} streptomycin, 1 mM PMSF pH 7.0).

The extract was further supplemented with a cocktail of protease inhibitors and subjected to ammonium sulfate fractionation (20–40% saturation) followed by 300 ml Q-Sepharose fast-flow column chromatography. After washing, crude vinculin was eluted with a linear (20–400 mM) KCl gradient.

The concentrated vinculin peak from the anion-exchange column was loaded onto a 530 ml Sephacryl S-300 column equilibrated with imidazole buffer (50 mM imidazole, 20 mM KCl, 1 mM EDTA, 1 mM EGTA, 1 mM PMSF pH 7.3). The proteins were fractionated using 600 ml of the imidazole buffer at 40 ml h^{-1}. As a final purification step, hydrophobic chromatography on TSK-gel (Toyopearl HW-65F) column with reverse (30–10% saturation) ammonium sulfate gradient was used; the final SDS–PAGE gel is shown in Fig. 1. Prior to crystallization, the protein was desalted by dialysis in Tris–HCl buffer pH 7.2 and concentrated by Microcon to 10 mg ml^{-1}.

2.2. Crystallization

To ensure the homogeneous size distribution of the protein molecules in the crystallization solution we have carried out dynamic light-scattering (DLS) spectroscopy, which is highly sensitive to the presence of impurities or aggregates compared with SDS–PAGE. The DLS experiments demonstrated that the preparation was monodisperse, with a monomodal distribution of size R_h = 4.7 nm and a polydispersity of 0.9∼1.0 nm, indicating that vinculin solution does not contain measurable impurities or aggregates.

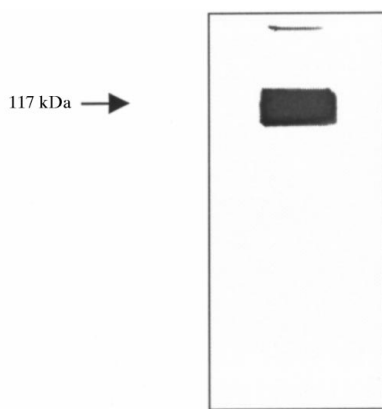Conditions for crystallization by the hanging-drop vapour-diffusion method were

Figure 1
10% SDS–PAGE gel, Coomassie blue staining. Vinculin peak after TSK-Gel column chromatography. Loading, 5 µg.
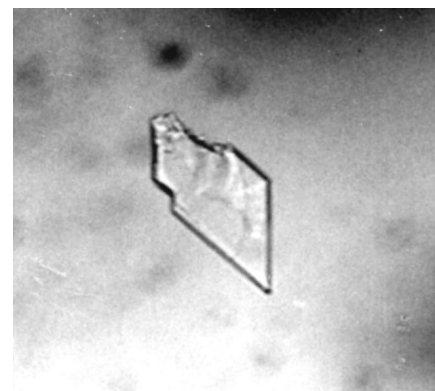

Figure 2
Photograph of a vinculin crystal obtained by the hanging-drop vapour-diffusion method. Dimensions are 0.3 × 0.3 × 0.05 mm.

initially screened by the use of the sparse-matrix approach (Crystal Screens I and II, Hampton Research, Laguna Hills, CA, USA). These experiments yielded two different crystallization conditions. Some very small single crystals in the form of needles were obtained with 30% PEG 4000 in 0.1 *M* Tris–HCl buffer pH 8.5. Refinement of the conditions did not improve the quality of these crystals. Crystals with thin plate morphology appeared in 1.8 *M* AS (ammonium sulfate, BDH) in 0.1 *M* MES [2-(*N*-morpholino)ethanesulfonic acid] buffer pH 6.5. After the initial crystallization conditions were established, optimization of several factors influencing crystal growth was conducted. Vinculin crystals of maximal size were obtained at 290 K from 5 µl drops containing 2 mg ml^{-1} protein, 0.9 *M* AS, 0.1 *M* MES pH 6.5 equilibrated against a reservoir of 1.8 *M* AS in 0.1 *M* MES buffer pH 6.5. Crystals appeared the next day as rhombic plates growing from one origin and continued to grow to their maximal size of 0.3 × 0.3 × 0.05 mm over an additional two weeks (see Fig. 2).

In view of the sensitivity of the vinculin to proteolytic degradation, we checked the presence of intact vinculin in the crystals. Individual crystals were removed from mother liqour, carefully washed several times with a reservoir solution and then dissolved in sample buffer. SDS–PAGE of dissolved crystals disclosed a single protein band with an apparent molecular weight of 117 kDa (Fig. 3).
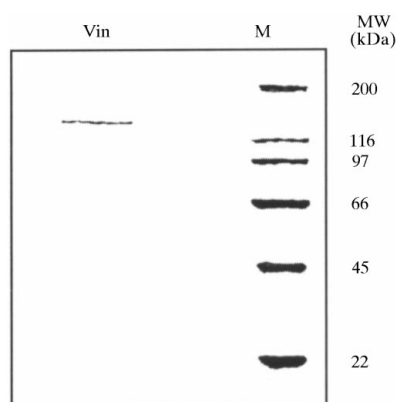
3. Preliminary results and discussion

Initial characterization of the crystals was carried out with an in-house Rigaku R-AXIS IIC image-plate detector mounted on a Rigaku FRC rotating-anode X-ray generator operating at 50 kV and 50 mA with monochromatic Cu *K*α (λ = 1.5418 Å) radiation and a 40 min exposure time. Data were collected at room temperature with a 0.5° oscillation angle and a crystal-to-detector distance of 123 mm and were processed using the program suite *HKL* 1.9.6 (Otwinowski & Minor, 1997). Results indicated that the crystals belong to a monoclinic space group *P*2₁ and have unit-cell parameters *a* = 57.8, *b* = 351, *c* = 70 Å, α = 90, β = 113.7, γ = 90° (Fig. 4). The crystals showed diffraction limit beyond 3.5 Å resolution at the X11 beamline at DESY at room temperature.

Assuming that the asymmetric unit contains one or two molecules of vinculin with a molecular mass of 117 kDa, the V_m value (Matthews, 1968) is calculated to be 5.48 or 2.47 Å³ Da^{-1}, resulting in a solvent content of the vinculin crystals of 77 and 55%, respectively.

Figure 3
SDS–PAGE analysis of vinculin crystals. The crystals of vinculin were dissolved in sample buffer and gel electrophoresis was performed. Vin, dissolved vinculin crystals; M, marker.
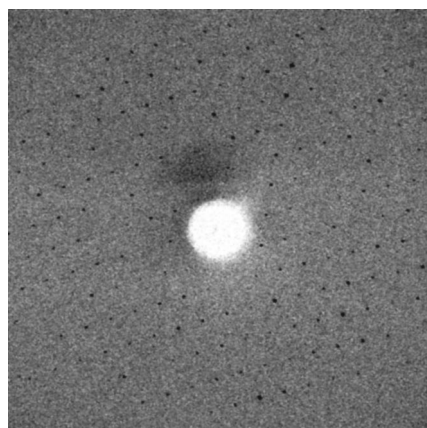

Figure 4
The oscillation photograph of a vinculin crystal taken using an R-AXIS IIC image plate. The oscillation range was 0.5° and the crystal-to-film distance was 123 mm. Outermost reflections are visible at 4.5 Å resolution.

References

Bakolista, T., de Pereda, J., Bagshaw, C., Critchley, D. & Liddington, R., (1999). *Cell*, **99**, 603–613.
Barstead, R. J. & Waterston, R. H. (1989). *J. Biol. Chem.* **264**, 10177–10185.
Ben-Ze'ev, A., Reiss, R., Bendori, R. & Gorodecki, B. (1990). *Cell Regul.* **1**, 621–636.
Brindle, N., Holt, M. K., Davies, J. E., Price, C. J. & Critchley, D. (1996). *Biochem. J.*, **318**, 753–757.
Burridge, K. & Mangeat, P. (1984). *Nature (London)*, **308**, 744–6.
Coutu, M. D. & Craig, S. W. (1988). *Proc. Natl Acad. Sci. USA*, **85**, 8535–8539.
Geiger, B. (1979). *Cell*, **18**, 193–205.
Geiger, B., Tokuyasu, K. T., Dutton, A. & Singer, S. J. (1980). *Proc. Natl Acad. Sci. USA*, **77**, 4127–4131.
Gimona, M., Furst, D. O. & Small, J. V. (1987). *J. Muscle Res. Cell Motil.* **8**, 329–341.
Hirsch, M. S., Law, L. Y., Trinkaus-Randall, V. & Svoboda, K. K. (1994). *Scanning*, **16**(5), 275–84.
Johnson, R. P. & Craig, S. W. (1995). *Biochem. Biophys. Res. Commun.* **210**, 159–164.
Johnson, R. P., Niggli, V., Durrer, P. & Craig, S. W. (1998). *Biochemistry*, **37**, 10211–10222.
Kioka, N., Sakata, S., Kawauchi, T., Amachi, T., Akiyama, S., Okazaki, K., Yaen, C., Yamada, K. & Aota, S. (1999). *J. Cell Biol.* **144**(1), 59–63.
Koteliansky, V. E., Gneushev, G. N., Glukhova, M. A., Venyaminov, S. Y. & Muzbek, L. (1984). *FEBS Lett.* **165**, 26–30.
Kroemker, M., Rudiger, A. H., Jockush, B. M. & Rudiger, M. (1994). *FEBS Lett.* **355**, 259–262.
Mandai, K., Nakanishi, H., Satoh, A., Takahashi, K., Satoh, K., Mishawka, H., Mizoguchi, A. & Takay, Y. (1999). *J. Cell Biol.* **144**(5), 1001–1017.
Matthews, B. W. (1968). *J. Mol. Biol.* **33**, 491–497.
Molony, L. & Burridge, K. (1985). *J. Cell Biochem.* **29**, 31–36.
Otto, J. J. (1990). *Cell Motil. Cytoskeleton*, **16**, 1–6.
Otwinowski, Z. & Minor, W. (1997). *Methods Enzymol.* **276**, 307–326.
Price, G. J., Jones, P., Davidson, M. D., Patel, B., Bendori, R., Geiger, B. & Critchey, D. R. (1989). *Biochem. J.* **259**, 453–461.
Price, G. J., Jones, P., Davidson, M. D., Patel, B., Eperon, I. C. & Critchley, D. R. (1987). *Biochem. J.* **245**, 595–603.
Schwienbacher, C., Jockush, B. M. & Rudiger, M. (1996). *FEBS Lett.* **384**, 71–74.
Sefton, B., Hunter, T., Ball, E. H. & Singer, S. J. (1981). *Cell*, **24**, 165–174.
Takubo, T., Hino, M., Suzuki, K. & Tatsumi, N. (1998). *Biotech. Histochem.* **73**, 310–315.
Turner, C. E., Glenney, J. R. & Burridge, K. (1990). *J. Cell Biol.* **111**, 1059–1068.
Weller, P. A., Ogryzko, E. P., Corben, E. B., Zhidkova, N. L., Patel, B., Price, G. J., Spurr, N. K., Koteliansky, V. E. & Critchley, D. R. (1990). *Proc. Natl Acad. Sci. USA*, **87**, 5667–5671.